

SUPPLEMENTAL MATERIAL

MiR-21 Lowers Blood Pressure in Spontaneous Hypertensive Rats by Up-regulating Mitochondrial Translation

Huaping Li¹, M.D.; Xiaorong Zhang², Ph.D.; Feng Wang¹, M.D., Ph.D.; Ling Zhou¹, M.D.; Zhongwei Yin¹, M.D.; Jiahui Fan¹, M.D.; Xiang Nie¹, M.D.; Peihua Wang¹, M.D., Ph.D.; Xiang-Dong Fu^{2,3}, Ph.D.; Chen Chen¹, M.D., Ph.D.; and Dao Wen Wang¹, M.D., Ph.D.

¹Division of Cardiology, Department of Internal Medicine, Tongji Hospital, Tongji Medical College, Huazhong University of Science and Technology, Wuhan 430030, China.

²Key Laboratory of RNA Biology, Institute of Biophysics, Chinese Academy of Sciences, Beijing 100101, China

³Department of Cellular and Molecular Medicine, University of California, San Diego, La Jolla, CA 92093-0651, USA; Institute of Genomic Medicine, University of California, San Diego, La Jolla, CA 92093-0651, USA.

Corresponding authors:

Chen Chen and Dao Wen Wang

Division of Cardiology, Department of Internal Medicine, Tongji Hospital, Tongji Medical College, Huazhong University of Science & Technology, 1095# Jiefang Ave., Wuhan 430030, China

Tel. & Fax: 86-27-8366-3280

Email: chenchen@tjh.tjmu.edu.cn; dwwang@tjh.tjmu.edu.cn

Expanded Methods

Cell culture and transfection

H9c2, HK2, HEK293T and HUVEC cells were maintained in DMEM with 10% FBS (Life Technologies, Carlsbad, CA). MiRNA mimics (50nM), inhibitors (50nM), siRNAs (50nM), and random small RNA controls (50nM) were transfected by Lipofectamine 2000 (Life Technologies, Carlsbad, CA). All of them used in the present study were purchased from Riobio Co., Ltd (Guangzhou, China).

Protein extraction and Western blotting

Protein concentrations were determined by the Bradford method. For Western blotting, total cell lysate was resolved by SDS-PAGE, transferred to nitrocellulose membrane, and blocked with 5% non-fat dry milk in TBS-T. The membrane was incubated with indicated primary antibody overnight at 4°C, followed by peroxidase-conjugated secondary antibody for 2 hours, and finally developed with the ECL system (Beyotime Institute of Biotechnology, Nanjing, China). Antibodies used in the present study were listed in Supplemental Table 1. Western blotting results were quantified by densitometry and processed with the ImageJ software (National Institutes of Health software).

RNA extraction and quantitative RT-PCR

Total RNA was isolated using TRIzol and reverse transcribed with

SuperScript[®] III First Strand Synthesis Kit (Life Technologies, Carlsbad, CA). Real-time PCR assays were performed with the SYBR[®] Select Master Mix (Life Technologies, Carlsbad, CA) on a 7900HT FAST Real-Time PCR System (Life Technologies, Carlsbad, CA) at 95°C for 10 min, 40 cycles at 95°C for 15 s in each cycle, and 60°C for 1 min in the final cycle. All reactions were performed in triplicate. The data were analyzed, as described¹. Primers used in the present study were listed in Supplemental Table 2.

RNA immunoprecipitation

Lysed mitochondria extracts were immunoprecipitated with anti-Ago2 antibody (Abnova Corporation, Taiwan, China) or IgG (Santa Cruz Biotechnology, Santa Cruz, CA) using protein G Sepharose beads (Santa Cruz Biotechnology, Santa Cruz, CA), as described². After elution from the beads, bound RNA were extracted with TRIzol and quantified by real time RT-PCR.

Study on human patients

In accordance with the Declaration of Helsinki and approved by the Ethics Committee of Tongji Hospital, 100 patients with hypertension and 120 controls were enrolled for the present study. All patients were admitted to Cardiovascular Division in Tongji Hospital between September 2012 and January 2016 and 5ml blood samples were collected via venous puncture after obtaining written informed consent. The clinical characteristics among patients

with hypertension in comparison with control subjects were listed in Supplemental Table 3. After centrifugation, the plasma were transferred to RNase-free tubes and stored at -80°C until analysis.

Application of recombinant adeno-associated virus (rAAV) to animals

All animal studies were conducted with the approval of the Animal Research Committee of Tongji Medical College, and in accordance with the NIH Guide for the Care and Use of Laboratory Animals. For in vivo experiments, male SHRs at 8 weeks of age (Vital River Laboratory Animal Technology Co., Ltd. Beijing, China) were divided into different groups (short term treatments: NS (saline), rAAV-GFP, rAAV-miR-21, rAAV-mut-miR-21, rAAV-anti-miR-21 and rAAV-mut-anti-miR-21, n=10; chronic treatments: rAAV-GFP, rAAV-miR-21, and rAAV-mut-miR-21, n=5). Rats in each group were injected with rAAV (5×10^{11} genome copies per rat) via tail vein using a modified hydrodynamic transfection method, as described previously³. Briefly, puncture of the lateral tail vein was performed with the rat lying on its right side and the base of the tail placed between the index and middle fingers; rAAV dissolved in saline was rapidly injected into the tail vein. Control rats were injected with an equal volume of saline. Treated SHRs were sacrificed (short term treatments: 4 week post injection; chronic treatments: 28 weeks post injection) and tissue samples were snap-frozen in liquid nitrogen or immediately processed for paraffin embedding. During this procedure,

anaesthetization of rats was performed with intraperitoneal injection of xylazine (5 mg/kg) and ketamine (80 mg/kg) mixture. To assess the adequacy of anesthesia during echocardiographic and hemodynamic examinations, parameters such as responsiveness, blood pressure, respiratory rate and heart rate were monitored. At the end of the procedure, animals were sacrificed by CO₂ inhalation, as previously described⁴.

Measurement of blood pressure and cardiac echocardiography

After rAAV injection, systolic blood pressures were measured every 4 weeks for 28 weeks at room temperature by a photoelectric tail-cuff system (PowerLab, AD Instrument Pty Ltd, Bella Vista, NSW, Australia), as described previously⁵.

Upon anesthetization, echocardiography was performed with VIVID 7 (General Electric, Milwaukee, WI) equipped with a 15-MHz linear array ultrasound transducer, as previously described⁶. To monitor LV catheterization, a catheter manometer (MPVS-400; Millar Instruments, Inc. Houston, TX) was inserted via the right carotid artery into the left ventricle. After stabilization for 20min, data were continuously recorded by using conductance data acquisition. Individual cardiac function parameters were calculated with the PVAN3.6 software (Millar Instruments, Inc. Houston, TX), as described previously⁷. For histological analysis, tissue sections were analyzed by light microscopy after hematoxylin-eosin staining, and the ImageJ program was

used to measure the area of each cell, as described⁸. Over 200 cardiomyocytes were measured per section.

Histological analysis

Formalin-fixed organs were embedded in paraffin and sectioned into 4 mm slices. The morphology and fibrosis were detected by HE and Sirius red staining, respectively. Tissue sections were visualized by microscope, and measured by mage-Pro Plus Version 6.0 (Media Cybernetics, Bethesda, MD, USA).

Supplemental Table 1. List of Antibodies.

Antibody	Company	Catalog number
Ago2	Abnova	H00027161-M01
NDUFA10	ABGENT	AP9768c
UQCRC1	ABGENT	AP18967a
mt-ND1	ABclonal	A5250
mt-Cytb	proteintech	55090-1-AP
mt-COI	BOSTER	BA4150
MRPL45	ABclonal	A5052
MRPS27	ABclonal	A4527
RPL4	ABclonal	A7620
RPS3	ABclonal	A2533
GW182	ABclonal	A6115
PTEN	ABclonal	A2113

Supplemental Table 2. List of PCR primers.

	Forward	Reverse
Rat-CYTB	5' CCCATTCATTATCGCCGC 3'	5' GGTGTTGAGGGGTTAGC 3'
Rat-ND1	5' GCTACATACTACGCAAAGGC 3'	5' TATTGAGGTGGTTAGGGGC 3'
Rat-COI	5' GCTCGTAAACCGTTGACTCT 3'	5' TCAGTTCCCGAAGCCTCC 3'
Rat-UQCRC1	5'CCAAGGACCTGCCAAAAGTT 3'	5' GGTGTGCCCTGGAATGCT 3'
Rat-GAPDH	5'ACAGCAACAGGGTGGTGGAC 3'	5'TTTGAGGGTGCAGCGAACTT 3'
Rat-BNP	5' TCTGCTCCTGCTTTTCCTTA 3'	5' GAACTATGTGCCATCTTGA 3'
Rat-12s RNA	5' ACTGGGATTAGATACCCCACTATG 3'	5'ATCGATTATAGAACAGGCTCCTC 3'
Rat-16s RNA	5' GTTATACCTTACCCCTTCTCGC 3'	5' CCCATTTCTTTCCGCTTCA 3'
Rat-5s RNA	5' GATCTCGGAAGCTAAGCAGG 3'	5' AAGCCTACAGCACCCGGTAT 3'
Rat-BNP	5' TCTGCTCCTGCTTTTCCTTA 3'	5' GAACTATGTGCCATCTTGA 3'

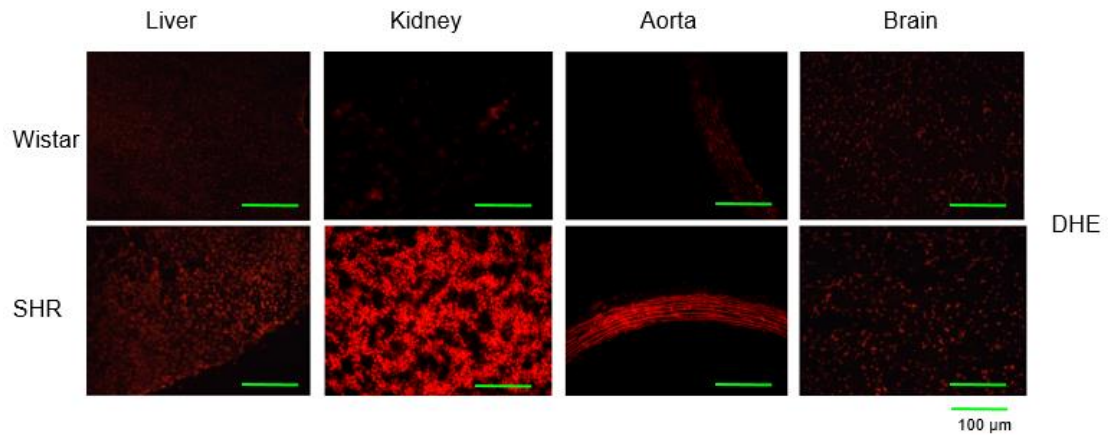
Supplemental Table 3. The clinical baseline characteristics of the hypertension patients.

Characteristics	Control (n=120)	Hypertension (n=100)	P value
Male/female (n/n)	60/60	50/50	1
Age (years)	53.9 ±0.97	53.6 ±1.31	0.805
BMI (kg/m ²)	23.9 ±0.43	24.9 ±0.36	0.073
SBP (mmHg)	118.8 ±1.06	158.3 ±1.62*	<0.001
DBP (mmHg)	73.9 ±0.87	91.9 ±1.27*	<0.001
Cr (mmol/L)	77.7 ±3.68	80.1 ±3.35	0.627
BUN (mmol/L)	5.82±0.28	5.80 ±0.22	0.953
Fasting glucose (mmol/L)	5.65 ±0.14	5.97 ±0.15	0.129
TG (mmol/L)	1.39±0.11	1.57 ±0.08	0.178
TC (mmol/L)	4.07±0.08	4.28±0.09	0.063
HDL (mmol/L)	1.08 ±0.03	1.07 ±0.03	0.915
LDL (mmol/L)	2.41 ±0.07	2.59 ±0.08	0.072

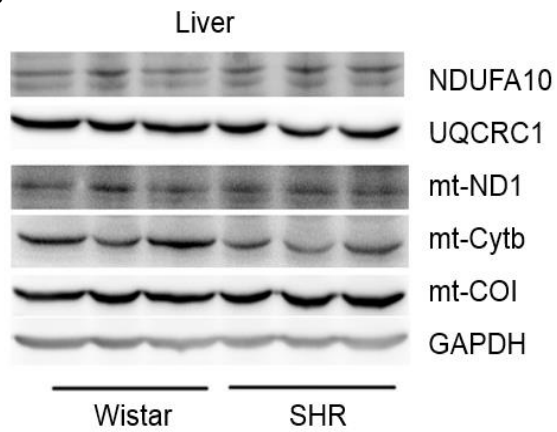
BMI, Body mass index; SBP, systolic blood pressure; DBP, diastolic blood pressure; Cr, Creatinine; BUN, Blood urea nitrogen; TG, Triglyceride; TC, total cholesterol; HDL, high-density lipoprotein; LDL, low-density lipoprotein; comparison among healthy control, hypertension patients with high blood pressure, and hypertension patients with normal blood pressure, Data were presented as mean ± SEM. *p<0.001 vs. control.

Supplemental Figure 1. Detection of ROS and expression of ETC subunits in various organs of Wistars and SHRs.

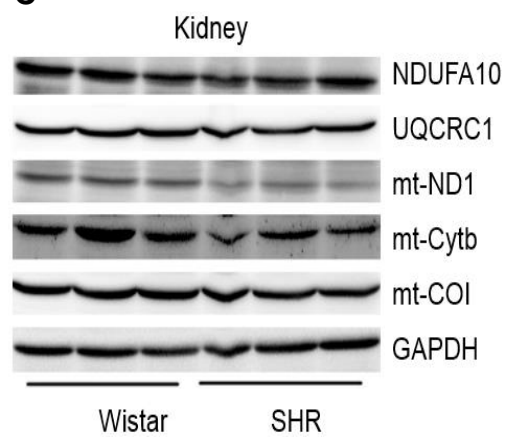
A



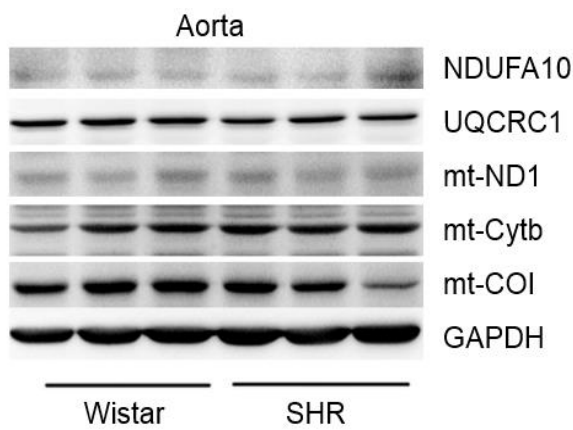
B



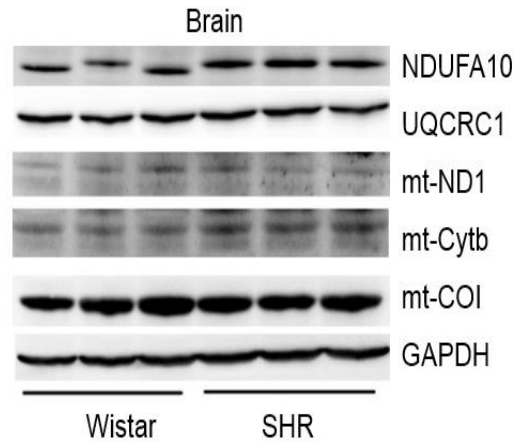
C

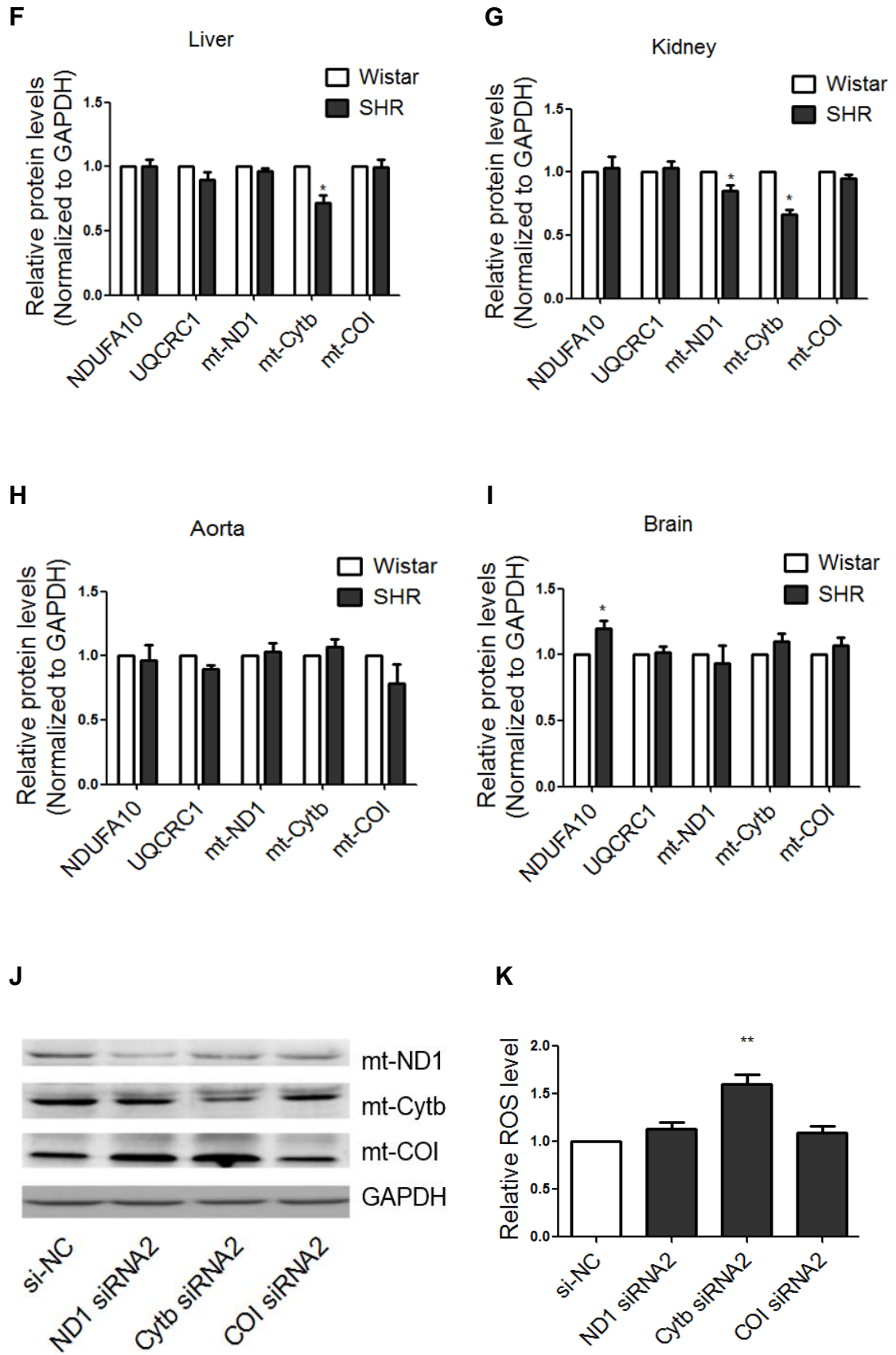


D



E



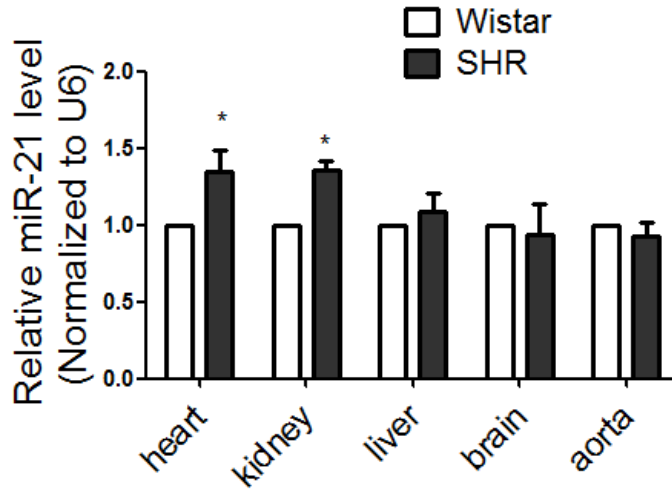


(A) Representative images of ROS detected by DHE probe in liver, kidney, aorta and brain sections of SHRs compared to Wistars. (B-I) Western blot

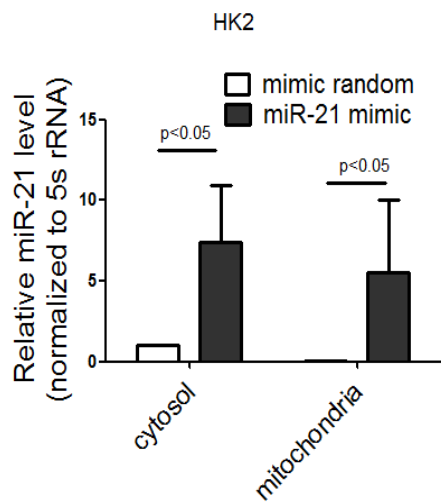
analysis of the ETC subunits in the liver, kidney, aorta and brain of SHRs. n=3, *p<0.05 compared to Wistars. (J) Protein levels of mitochondrial subunits in H9c2 cells transfected with the indicated siRNAs. (K) ROS levels in H9c2 cells transfected with si-ND1, si-Cytb or si-COI. n=3, **p<0.01 related to si-NC.

Supplemental Figure 2. MiR-21 enhanced translation of Cytb into the mitochondria.

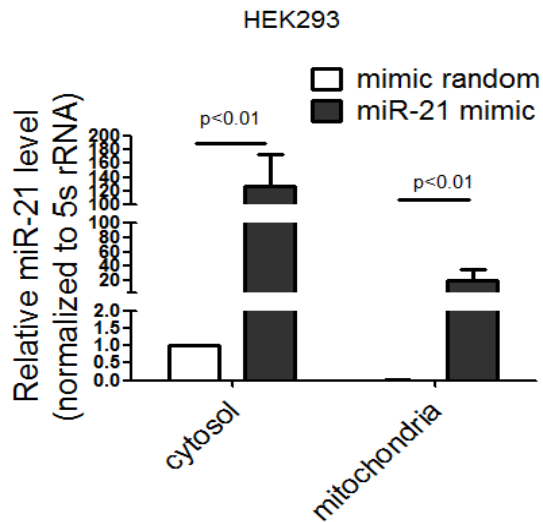
A



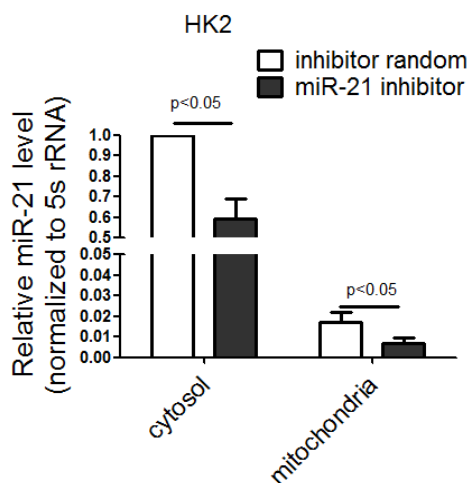
B



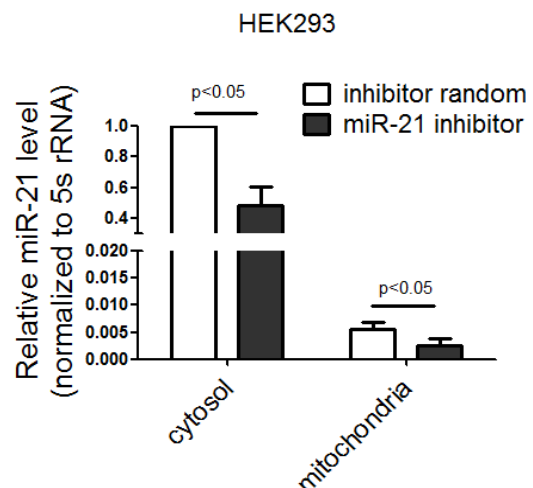
C

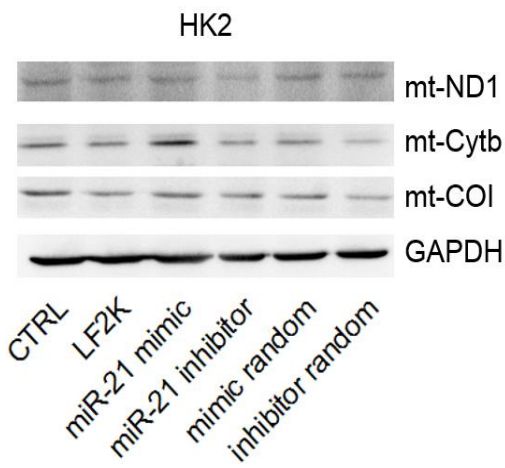
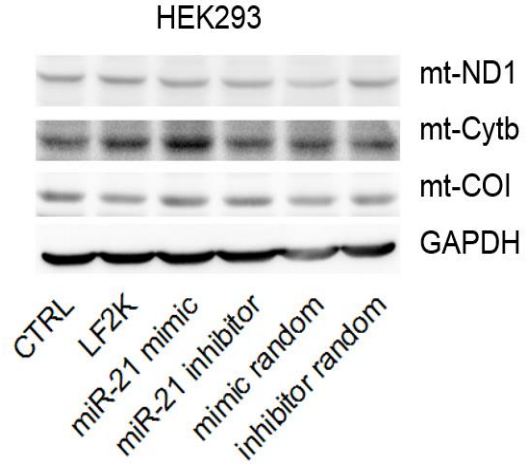
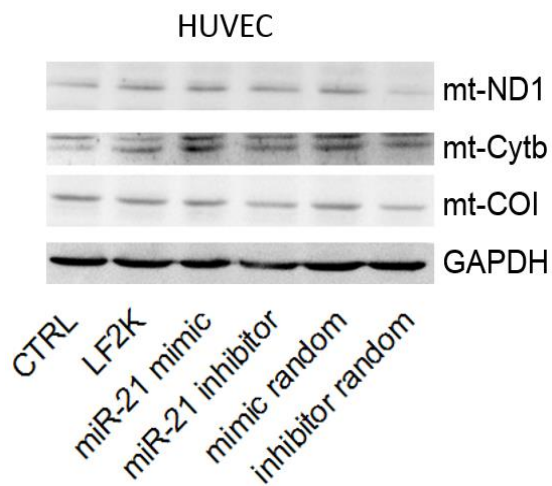
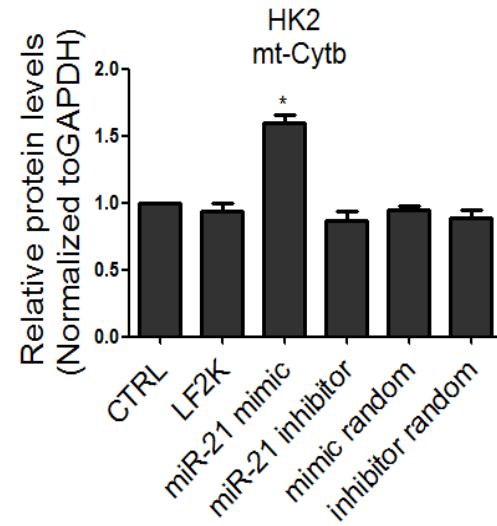
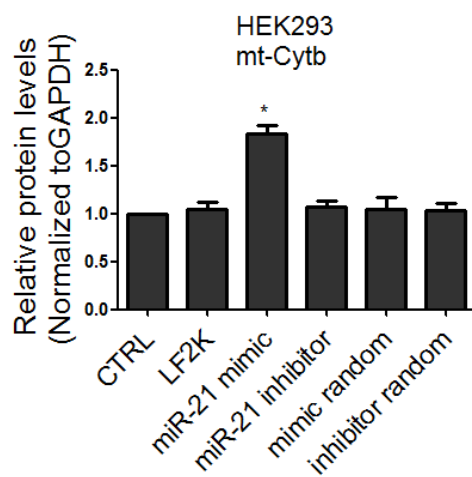
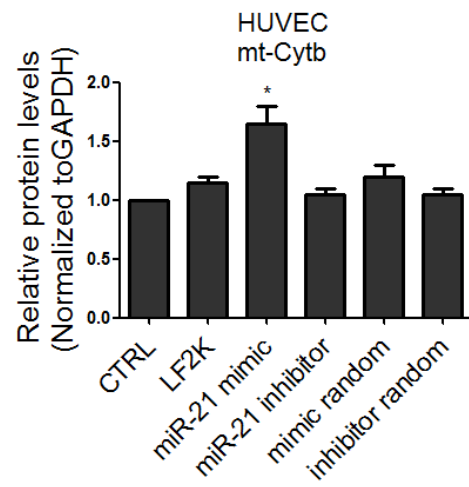


D



E



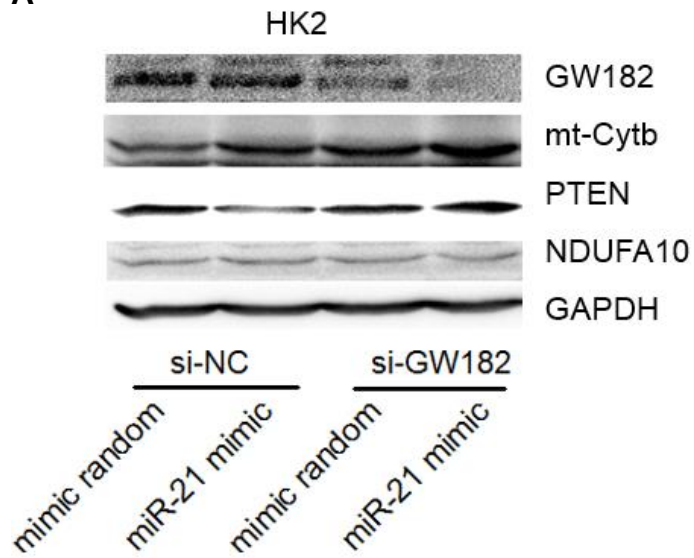
F**G****H****I****J****K**

(A) Total miR-21 levels in different tissue of SHR and Wistar. n=3, *p<0.05.

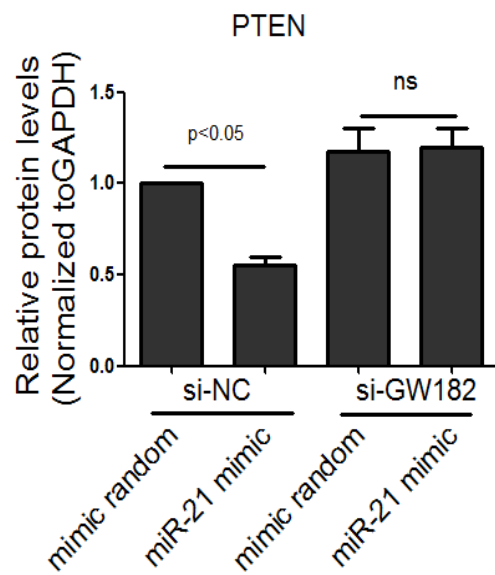
(B-E) MiR-21 levels in the cytosol and mitochondria of transfected HK2 and HEK293 cells. n=3. (F-K) Effects of miR-21 on the protein expressions of mitochondrial subunits. n=3, *p<0.05.

Supplemental Figure 3. Effects of miR-21 on Cytb and PTEN expression by knocking down GW182.

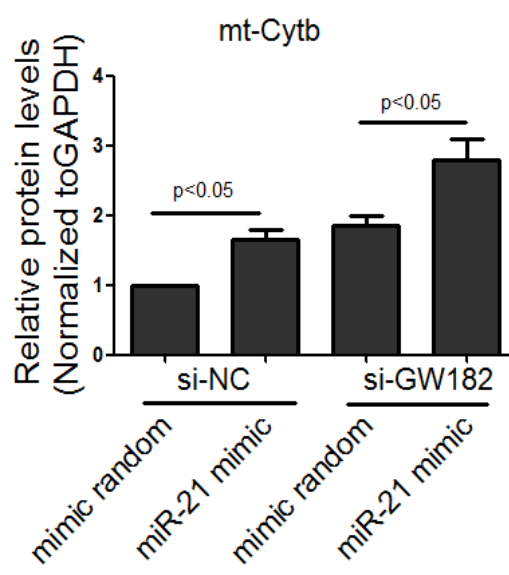
A

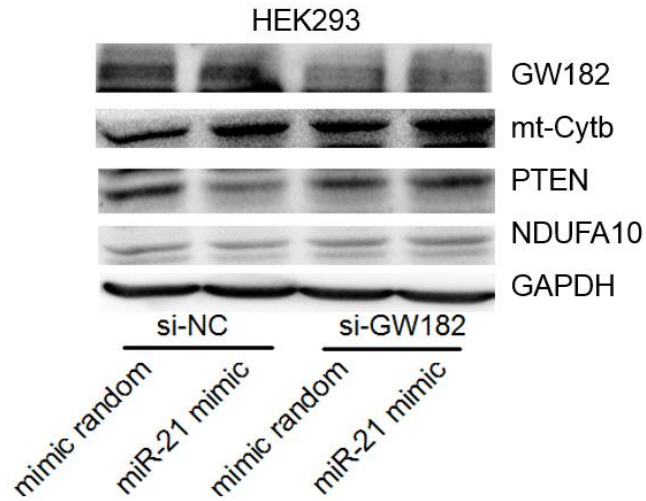
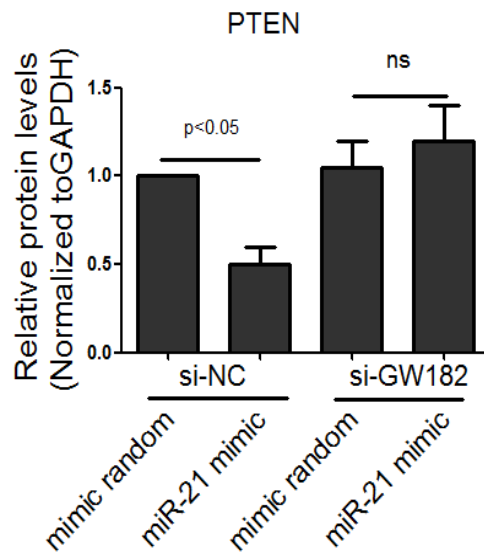
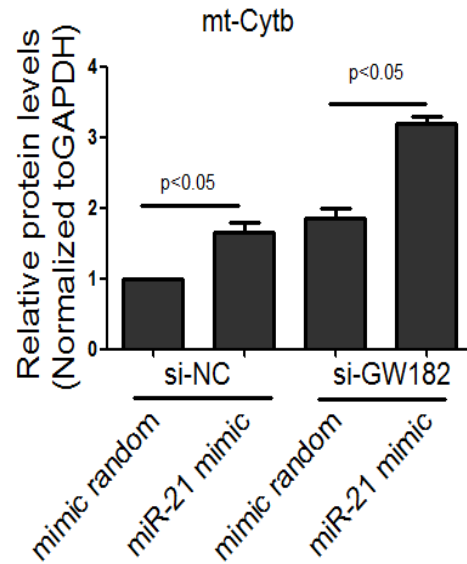


B



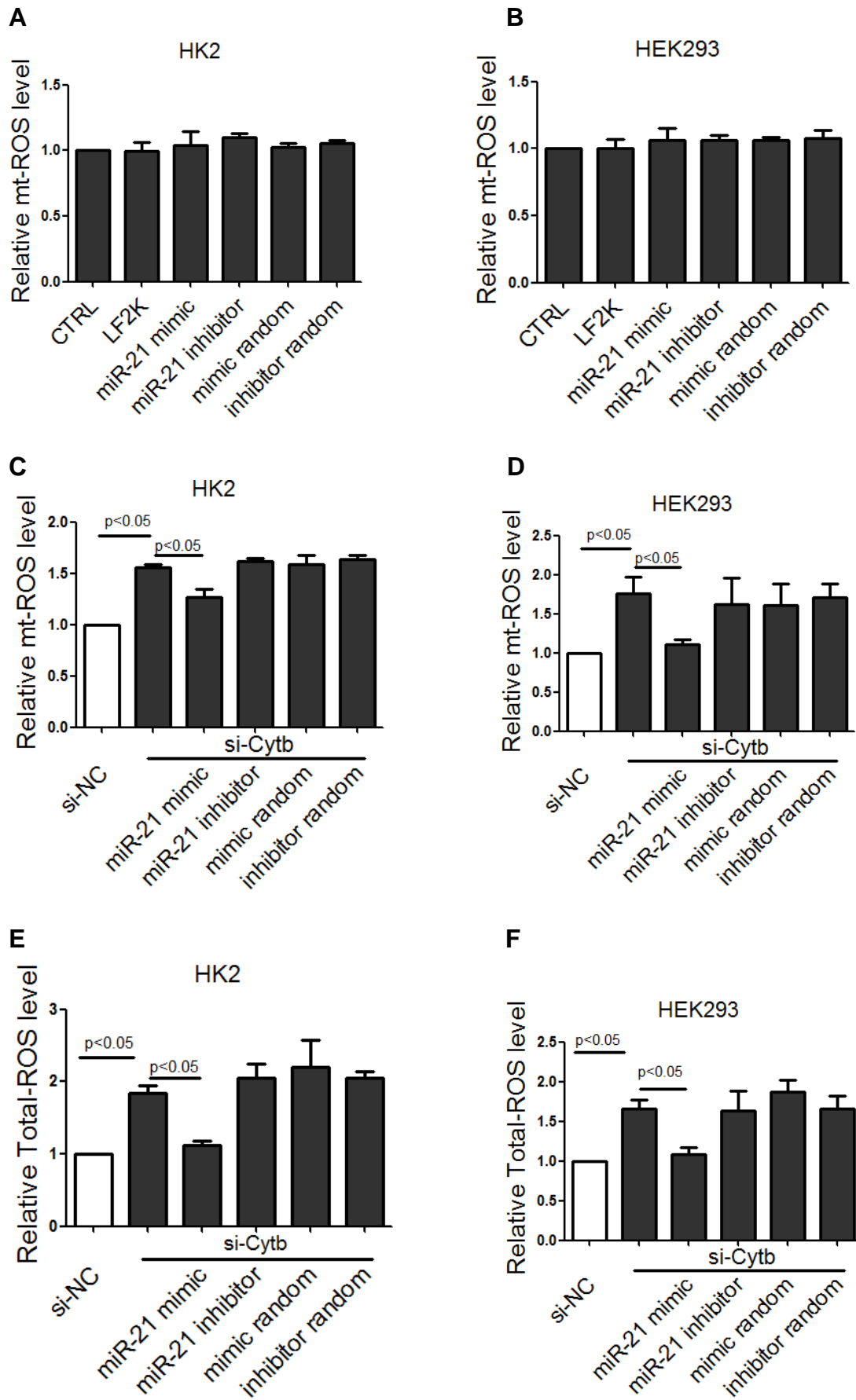
C



D**E****F**

(A-C) Effects of miR-21 on Cytb and PTEN in HK2 cells. (D-F) Effects of miR-21 on Cytb and PTEN in HEK293 cells. $n=3$.

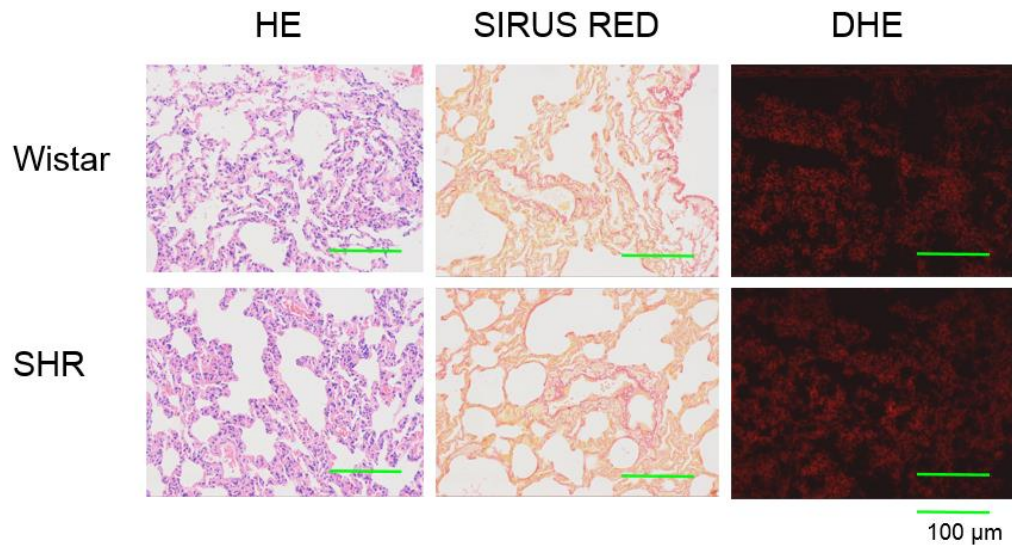
Supplemental Figure 4. Effects of miR-21 on ROS.



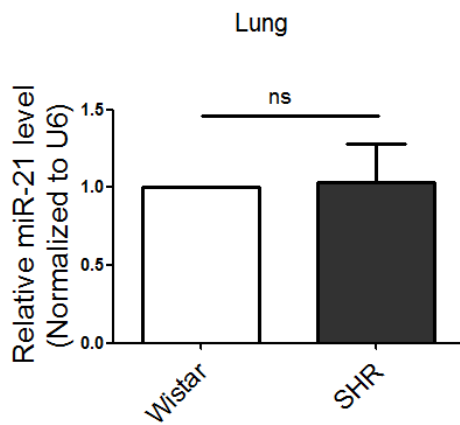
(A) Effects of miR-21 on mt-ROS in HK2 cells. (B) Effects of miR-21 on mt-ROS in HEK293 cells. (C) Effects of miR-21 on mt-ROS in si-Cytb treated HK2 cells. (D) Effects of miR-21 on mt-ROS in si-Cytb treated HEK293 cells. (E) Effects of miR-21 on total-ROS in si-Cytb treated HK2 cells. (F) Effects of miR-21 on total-ROS in si-Cytb treated HEK293 cells. n=3.

Supplemental Figure 5. Morphology, miR-21 levels and expression of ETC subunits in lungs of Wistars and SHRs.

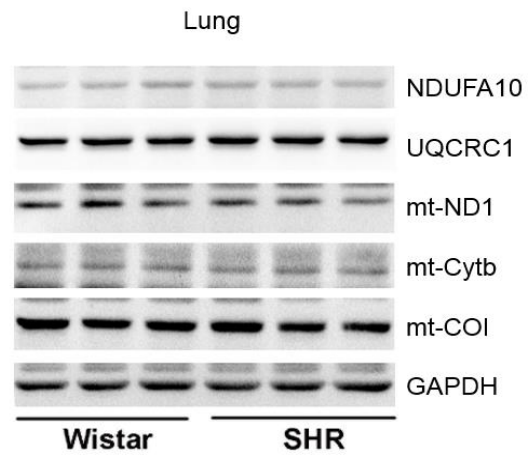
A



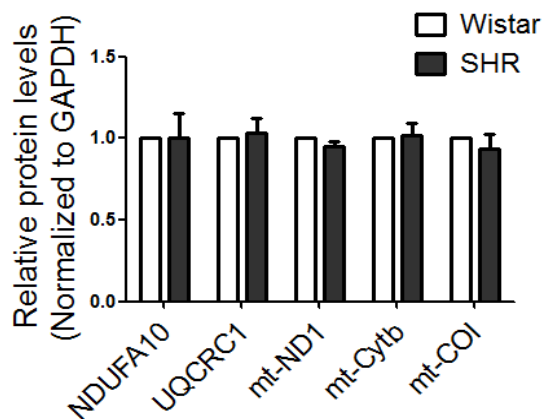
B



C

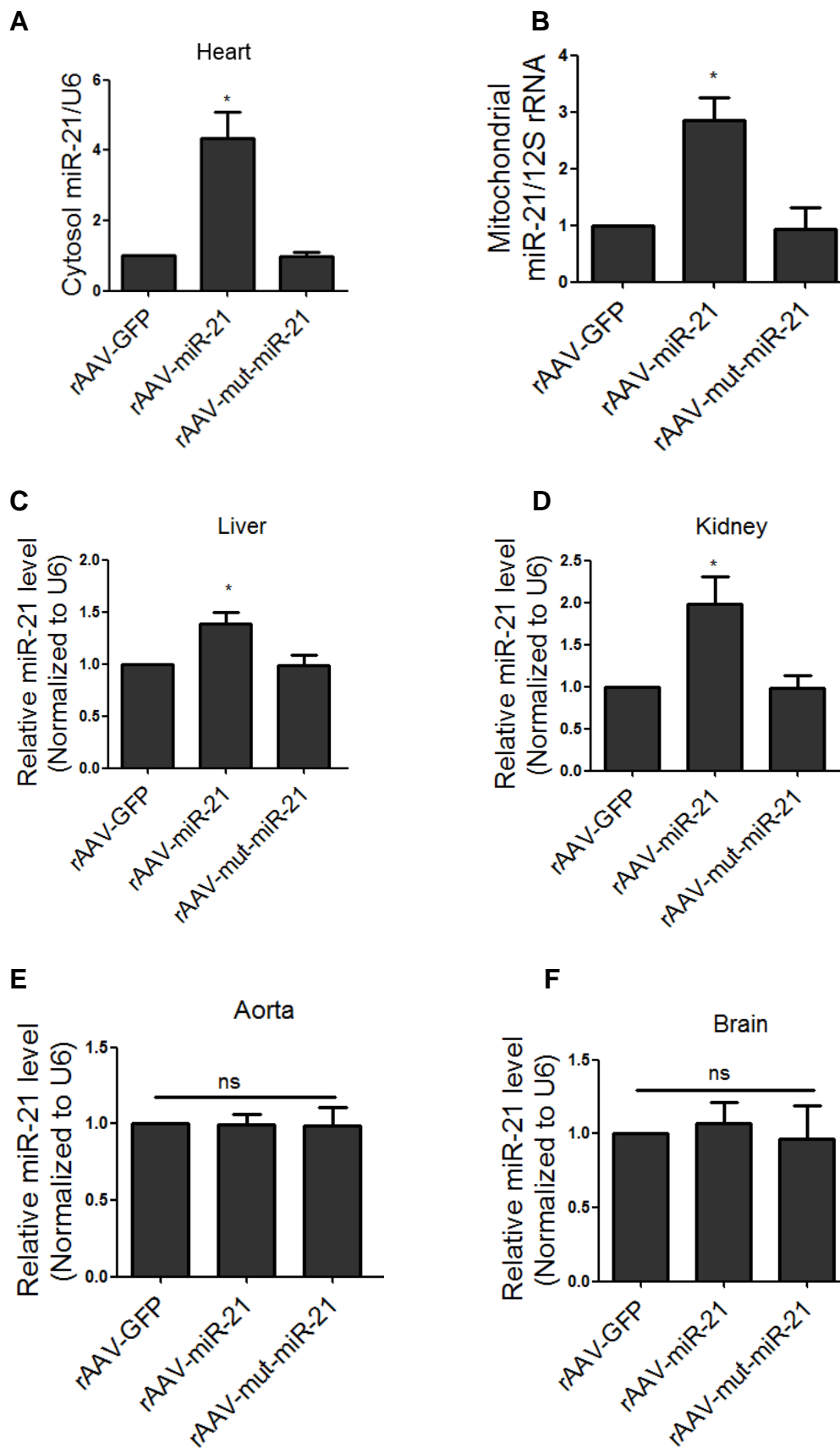


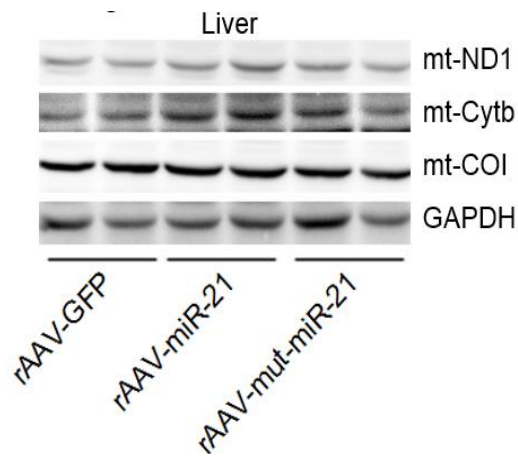
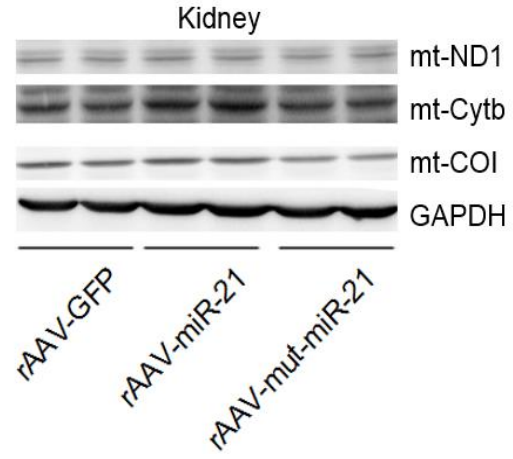
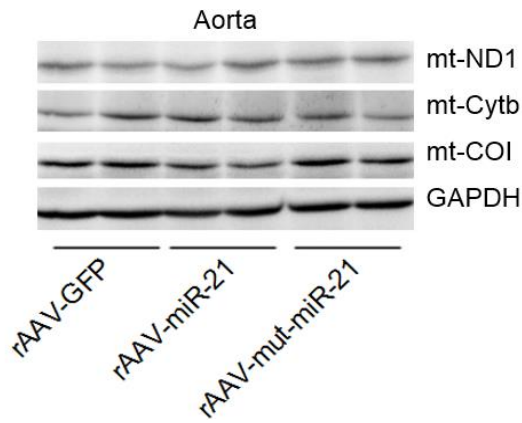
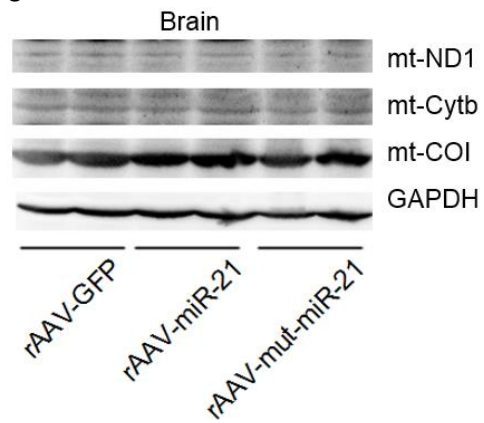
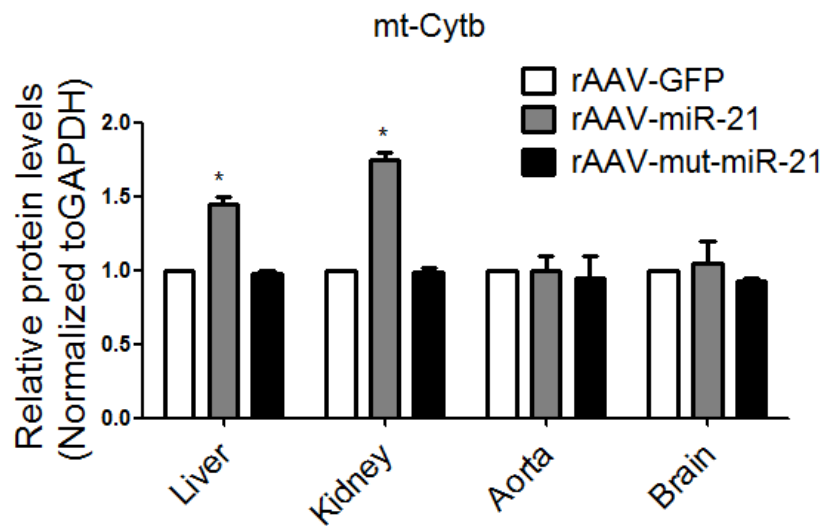
D

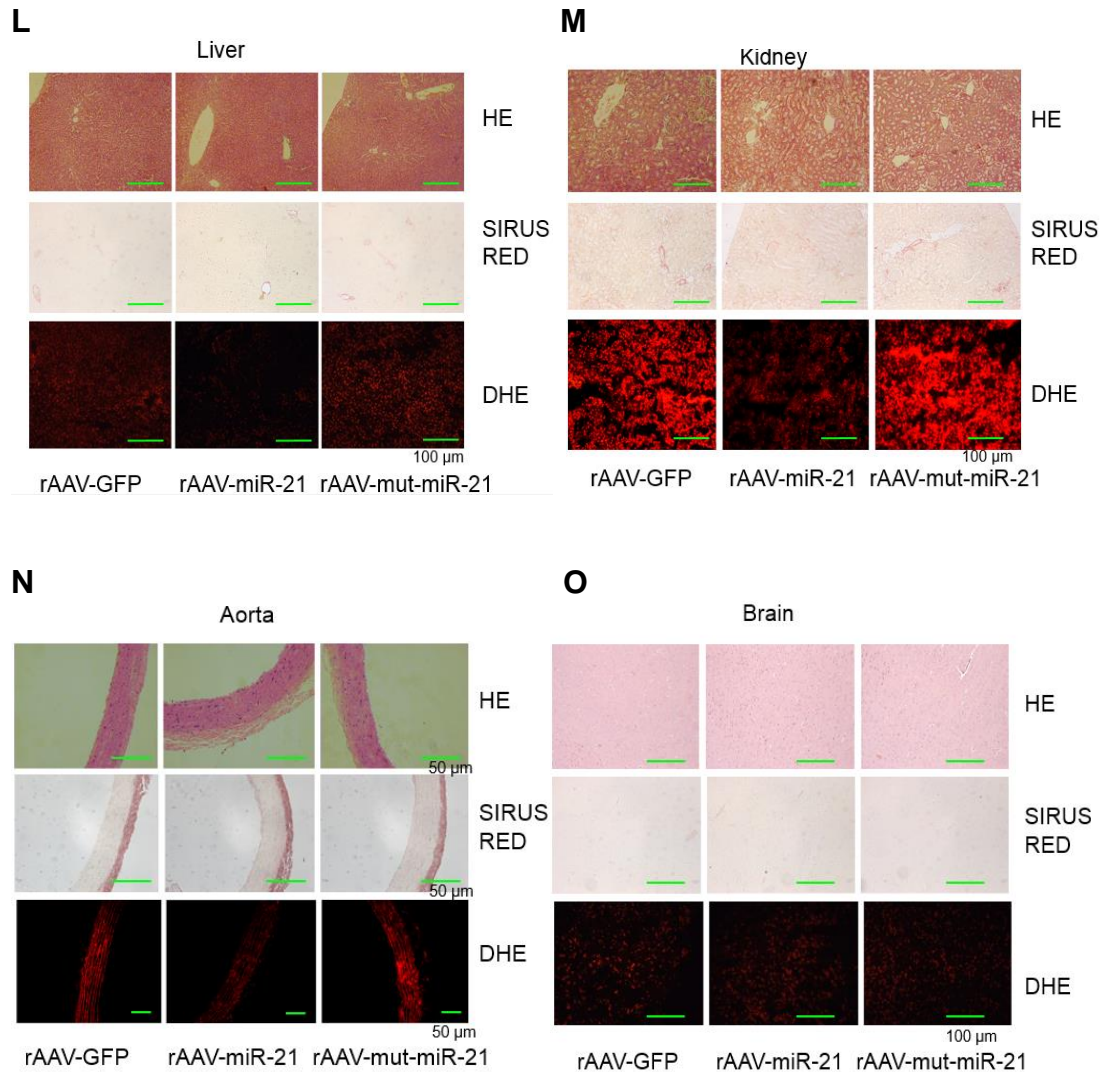


(A) Representative images of morphology, fibrosis and ROS in lung sections of SHRs compared to Wistars. (B) miR-21 level in lung of SHRs compared to Wistars. (C-D) Western blotting analysis of the ETC subunits in lung tissues. n=3, *p<0.05

Supplemental Figure 6. Effects of long-term rAAV-miR-21 treatments in various organs of SHR.

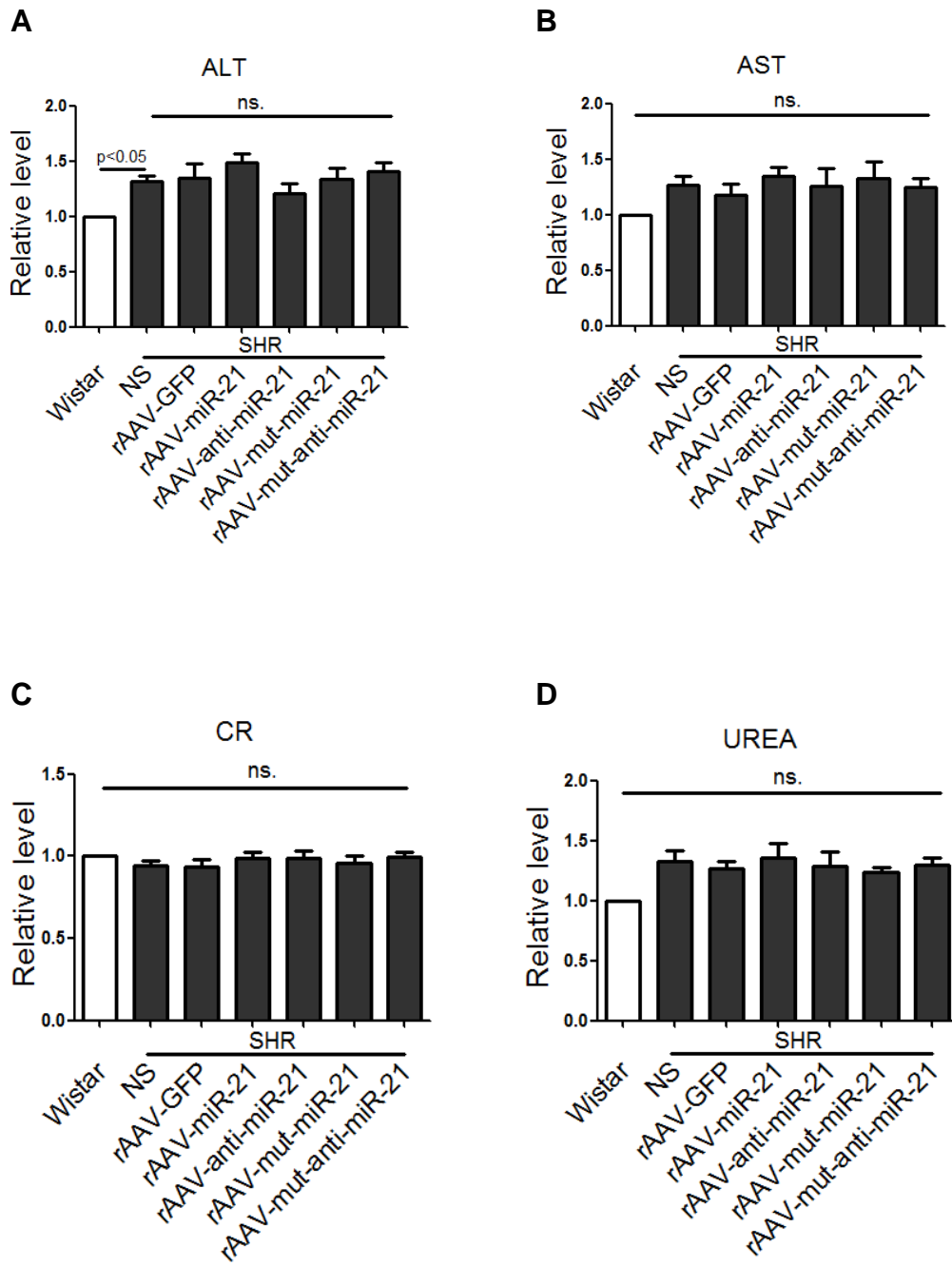


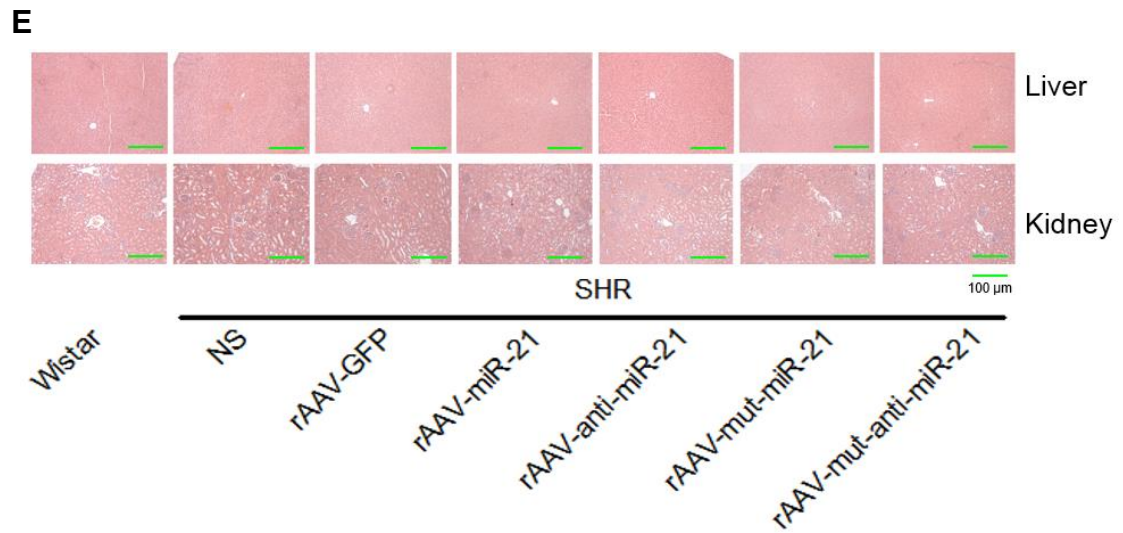
G**H****I****J****K**



(A, B) Levels of miR-21 in cytosol and mitochondria of SHR hearts. $n=5$, $**p<0.01$ vs. rAAV-GFP. (C-F) MiR-21 levels in liver, kidney, aorta and brain of various groups. (G-K) Western blotting analysis of Cytb protein in liver, kidney, aorta and brain of various groups. (L-O) Representative images of HE staining, Sirius Red staining and DHE of liver, kidney, aorta and brain of various groups. All data were presented as mean \pm SEM, $n=5$, $*p<0.05$, $**p<0.01$.

Supplemental Figure 7. Effects of short-term rAAV-miR-21 treatments on function and morphology of liver and kidney.





(A-D) Plasma AST, ALT, CR and UREA in various groups. (E) Representative images of HE staining of liver and kidney in various groups. n=10.

References

1. Chen C, Ridzon DA, Broomer AJ, Zhou Z, Lee DH, Nguyen JT, Barbisin M, Xu NL, Mahuvakar VR, Andersen MR, Lao KQ, Livak KJ, Guegler KJ. Real-time quantification of micrnas by stem-loop rt-pcr. *Nucleic Acids Res.* 2005;33:e179
2. Beitzinger M, Meister G. Experimental identification of microrna targets by immunoprecipitation of argonaute protein complexes. *Methods Mol Biol.* 2011;732:153-167
3. Song E, Lee SK, Wang J, Ince N, Ouyang N, Min J, Chen J, Shankar P, Lieberman J. Rna interference targeting fas protects mice from fulminant hepatitis. *Nat Med.* 2003;9:347-351
4. Yang S, Chen C, Wang H, Rao X, Wang F, Duan Q, Chen F, Long G, Gong W, Zou MH, Wang DW. Protective effects of acyl-coa thioesterase 1 on diabetic heart via pparalpha/pgc1alpha signaling. *PLoS One.* 2012;7:e50376
5. Xiao B, Li X, Yan J, Yu X, Yang G, Xiao X, Voltz JW, Zeldin DC, Wang DW. Overexpression of cytochrome p450 epoxygenases prevents development of hypertension in spontaneously hypertensive rats by enhancing atrial natriuretic peptide. *J Pharmacol Exp Ther.* 2010;334:784-794
6. Ma F, Lin F, Chen C, Cheng J, Zeldin DC, Wang Y, Wang DW. Indapamide lowers blood pressure by increasing production of epoxyeicosatrienoic acids in the kidney. *Mol Pharmacol.* 2013;84:286-295
7. Xu X, Wan W, Ji L, Lao S, Powers AS, Zhao W, Erikson JM, Zhang JQ. Exercise training combined with angiotensin ii receptor blockade limits post-infarct ventricular remodelling in rats. *Cardiovasc Res.* 2008;78:523-532
8. Rangan GK, Tesch GH. Quantification of renal pathology by image analysis. *Nephrology (Carlton).* 2007;12:553-558